

SUPPORTING INFORMATION for

2-Hydroxyterpenylic acid: An oxygenated marker compound for α -pinene secondary organic aerosol in ambient fine aerosol

*Ariane Kahnt¹, Yoshiteru Iinuma², Frank Blockhuys³, Anke Mutzel², Reinhilde Vermeulen¹,
Tadeusz E. Kleindienst⁴, Mohammed Jaoui⁵, John H. Offenberg⁴, Michael Lewandowski⁴,
Olaf Böge², Hartmut Herrmann², Willy Maenhaut^{1,6}, and Magda Claeys^{1,*}*

¹Department of Pharmaceutical Sciences, University of Antwerp, Campus Drie Eiken,
BE 2610 Antwerp, Belgium

²Leibniz-Institut für Troposphärenforschung (TROPOS), Permoserstr. 15,
D 04318, Leipzig, Germany

³Department of Chemistry, University of Antwerp, Campus Drie Eiken,
BE 2610 Antwerp, Belgium

⁴National Exposure Research Laboratory, Office of Research and Development, United States
Environmental Protection Agency, Research Triangle Park, NC 27711, USA

⁵Alion Science and Technology, Research Triangle Park, NC 27711, USA

⁶Department of Analytical Chemistry, Ghent University, Krijgslaan 281, S12,
BE 9000 Ghent, Belgium

*Correspondence to: magda.claeys@uantwerpen.be

This pdf file includes:

Additonal information on the time-resolved α -pinene/NO_x/air irradiation experiment, Figures
S1 to S16, and explanation of the Figures.

S1. Temporal evolution of the major 2-hydroxyterpenylic acid 2R, 3R diastereoisomer

Chamber aerosol samples

Eight filter samples were collected during the time-resolved α -pinene photooxidation experiment in the EPA chamber, where the first GF1 filter sample represents a background sample, which was collected before the lights were turned on. The other filter samples were collected during the irradiation at the following median experimental times: 0.5 (GF2), 1.6 (GF3), 2.7 (GF4), 3.9 (GF5), 5 (GF6), 6.1 (GF7), and 7.2 (GF8) hours. Ozone formation was observed first at about 2.5 hours, and α -pinene was completely consumed after 3.8 h of irradiation. The aerosol samples were collected on 47-mm Zefluor filter (Pall Gelman Laboratory, Ann Arbor, MI, USA) and the filters were weighed before and after the sampling to determine the SOA mass gravimetrically. The filters were kept afterwards in a freezer at -25 °C until the further sample preparation and the chromatographic analysis were performed. One half was cut of each filter sample and the halves were weighed to determine the SOA fraction used for subsequent extraction and analysis. The filter extraction was performed as described for the campholenic aldehyde ozonolysis (CAO) SOA sample in the Experimental Section of the main text. The final reconstitution volume was 250 μ L methanol/water (50/50, v/v) and the filters were analyzed by LC/(–)ESI-ITMS.

The time evolution of the oxidation products detected at m/z 157, 171, 183, 185, 187, 203 and 231 was investigated and the following compounds were used for their quantification: terebic acid [m/z 157, retention time (RT) 17.3 min], terpenylic acid (m/z 171, RT 19.1 min), *cis*-pinonic acid (m/z 183, RT 23.2 min), *cis*-pinic acid (m/z 185, RT 22.2 min), MBTCA (m/z 203, RT 19.1 min), and diaterpenylic acid acetate (m/z 231, RT 21.8 min). The MW 188 compound eluting at 16.4 min, assigned to the 2-hydroxyterpenylic acid 2R,3R diastereoisomer, was quantified using terpenylic acid as a surrogate standard.

Temporal evolution of the 2-hydroxyterpenylic acid 2R,3R diastereoisomer

The temporal evolution of the 2-hydroxyterpenylic acid 2R,3R diastereoisomer and of other known oxidation products is summarized in Figure S1, together with the SOA mass formation as a function of irradiation time.

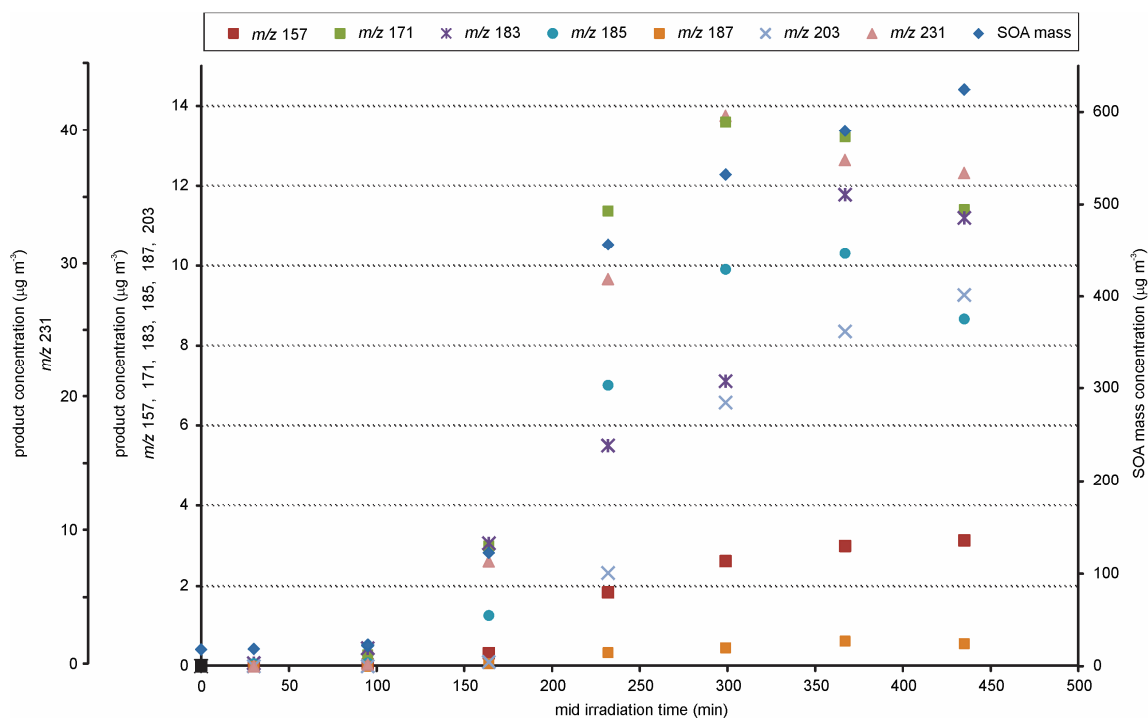


Figure S1. Evolution of terebic acid (m/z 157), terpenylic acid (m/z 171), *cis*-pinonic acid (m/z 183), *cis*-pinic acid (m/z 185), 2-hydroxyterpenylic acid (m/z 187), MBTCA (m/z 203), diaterpenylic acid acetate (m/z 231) from LC/(-)ESI-MS analysis, and of the SOA mass during an α -pinene/ NO_x /air photooxidation experiment as a function of irradiation time. All the provided mass concentrations are corrected for wall losses.

S2. Formation pathways for 2-hydroxyterpenylic acid

Formation pathways for 2-hydroxyterpenylic acid through α -pinene ozone and OH reactions are summarized in Figure S2.

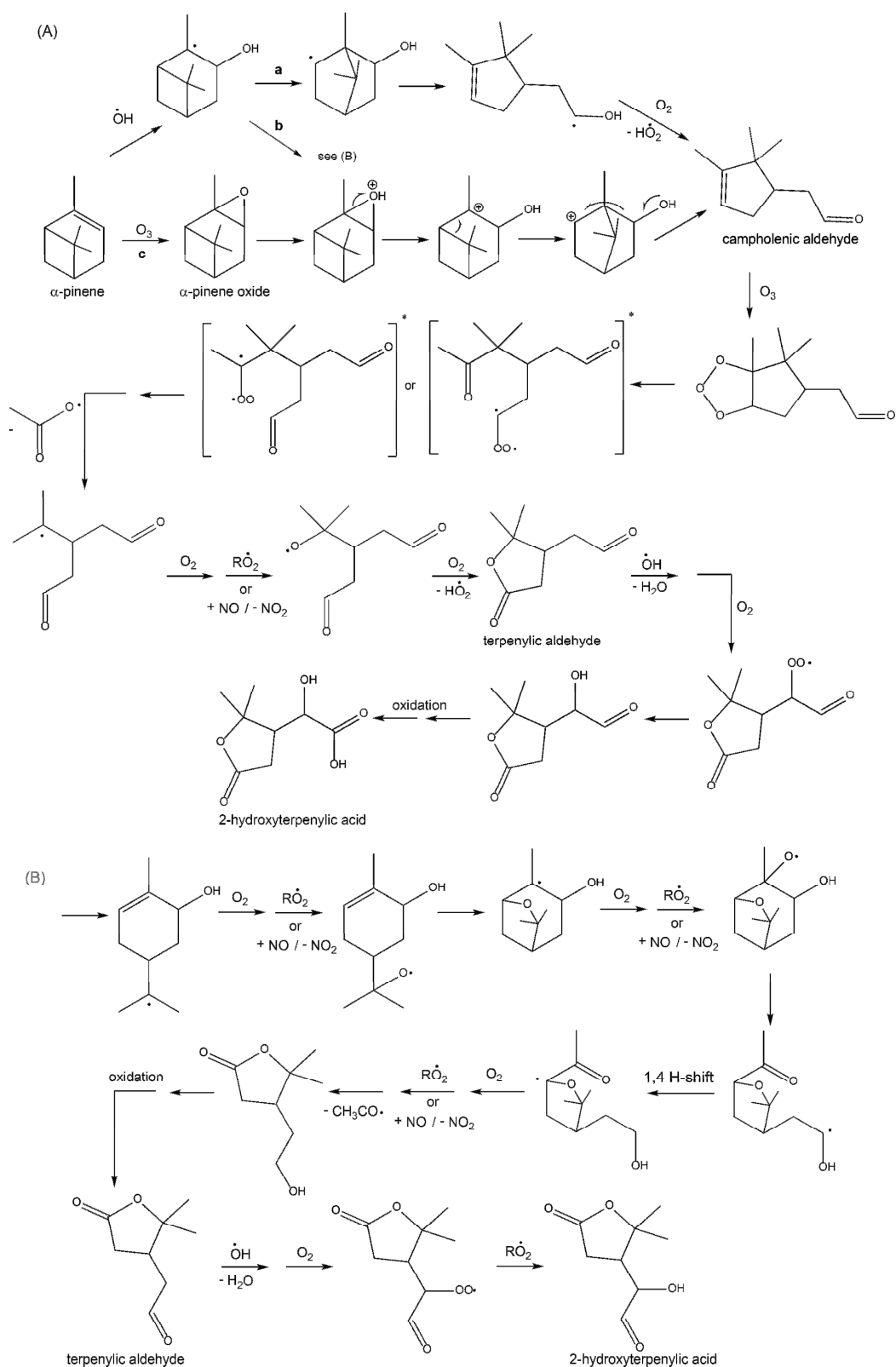


Figure S2. Proposed formation mechanisms for 2-hydroxyterpenylic acid from (A) α -pinene ozonolysis and (B) the α -pinene OH reaction. The pathways shown here were adapted from the literature and further extended: **a** from Claeys et al., 2009 (1), **b** from Van den Bergh et al., 2000 (2), and **c** from Inuma et al., 2013 (3) and Kahnt et al., 2014 (4).

S3. Characterization of MW 188 compounds using LC/ESI-ITMS analysis

Based on matching RT (16.4 min) and the similarity of the MS data with those obtained for CAO SOA and the ambient sample (Fig. 1), it can be concluded that the same 2-hydroxyterpenylic acid diastereoisomer is present in the α -pinene/OH SOA sample (Fig. S3). However, only small amounts of this compound were present in this sample, indicating that the crucial reaction conditions to produce this compound are not met during the chamber experiment.

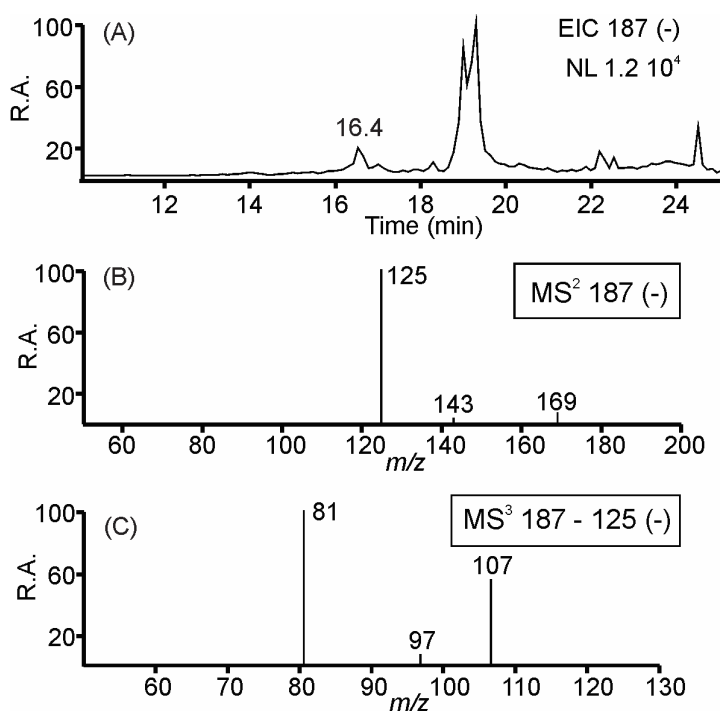


Figure S3. Selected LC/(-)ESI-ITMS data for the α -pinene/OH SOA sample: (A) m/z 187 extracted ion chromatogram (EIC); and selected MS data for the compound eluting at 16.4 min: (B) m/z 187 MS^2 spectrum and (C) m/z 187 \rightarrow m/z 125 MS^3 spectrum. Abbreviation: NL, normalization level.

Possible fragmentation pathways for the proposed 2-hydroxyterpenylic acid (MW 188) diastereoisomers, based on the detailed interpretation of (-)ESI- MS^n data (Fig. 1), are summarized in Figure S4.

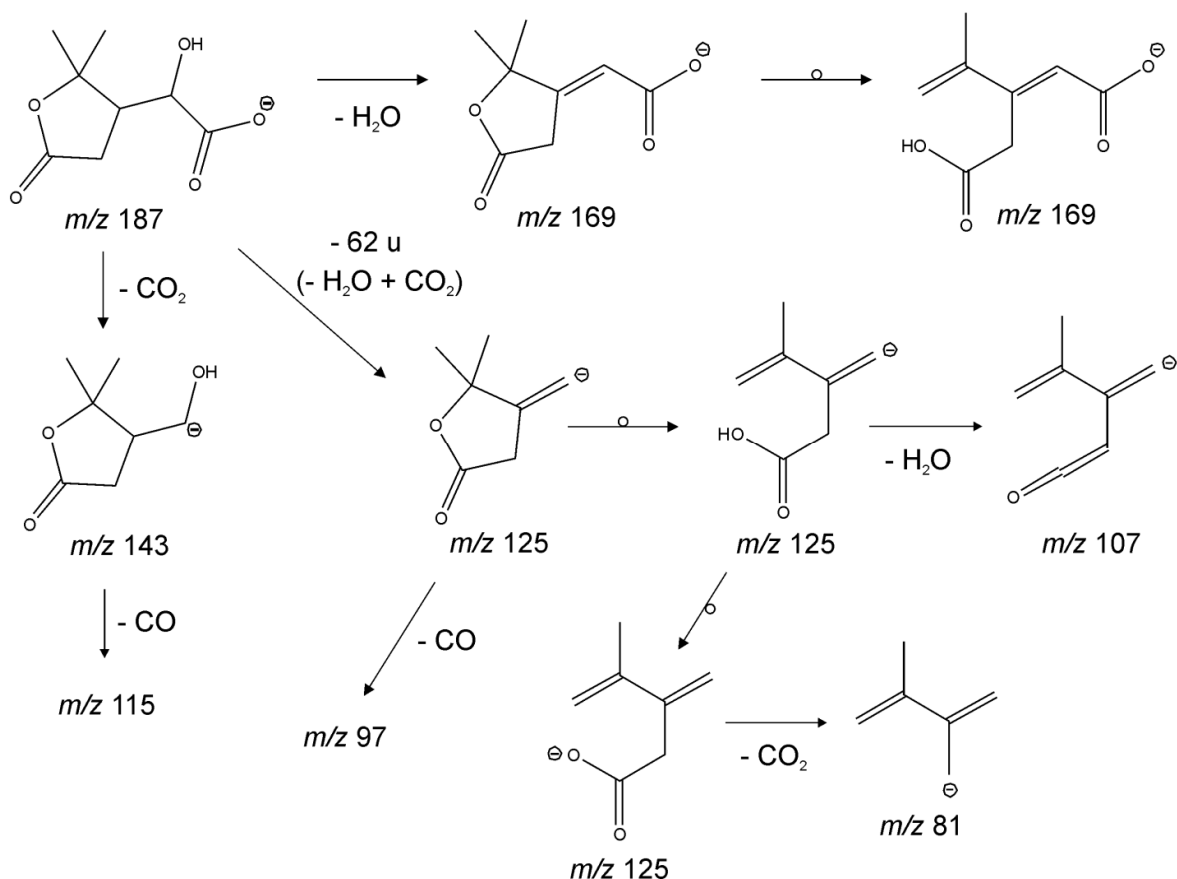


Figure S4. Possible fragmentation pathways for 2-hydroxyterpenylic acid on the basis of LC/(–)ESI-ITMS data.

Figure S5 presents selected MS data for the protonated forms of the authentic standards terebic acid, terpenylic acid, and the MW 188 compounds, attributed to 2-hydroxyterpenylic acid diastereoisomers, which occur in CAO SOA and the ambient sample. Protonated terebic and terpenylic acid readily lose a molecule of water resulting in m/z 141 and m/z 155, respectively [Fig. S5(A, C)]. Further fragmentation of m/z 141 mainly results in m/z 123 and m/z 113 [Fig. S5(B)], corresponding to the loss of a molecule of water and CO, respectively. On the other hand, further fragmentation of m/z 155 mainly results in m/z 127, owing to the loss of CO [Fig. S5(D)]. As expected, the protonated forms of 2-hydroxyterpenylic acid show the sequential loss of two molecules of water resulting in product ions at m/z 171 and m/z 153 [Fig. S5(E-H)], fully in line with the proposed 2-hydroxyterpenylic acid structure. Again, it can be noted that the MS data obtained for the two MW 188 compounds present in the CAO SOA sample are very similar and only differ by the relative abundances of minor product ions as observed from (–)ESI-ITMS data [Fig. 1 (C-F)], consistent with diastereoisomers.

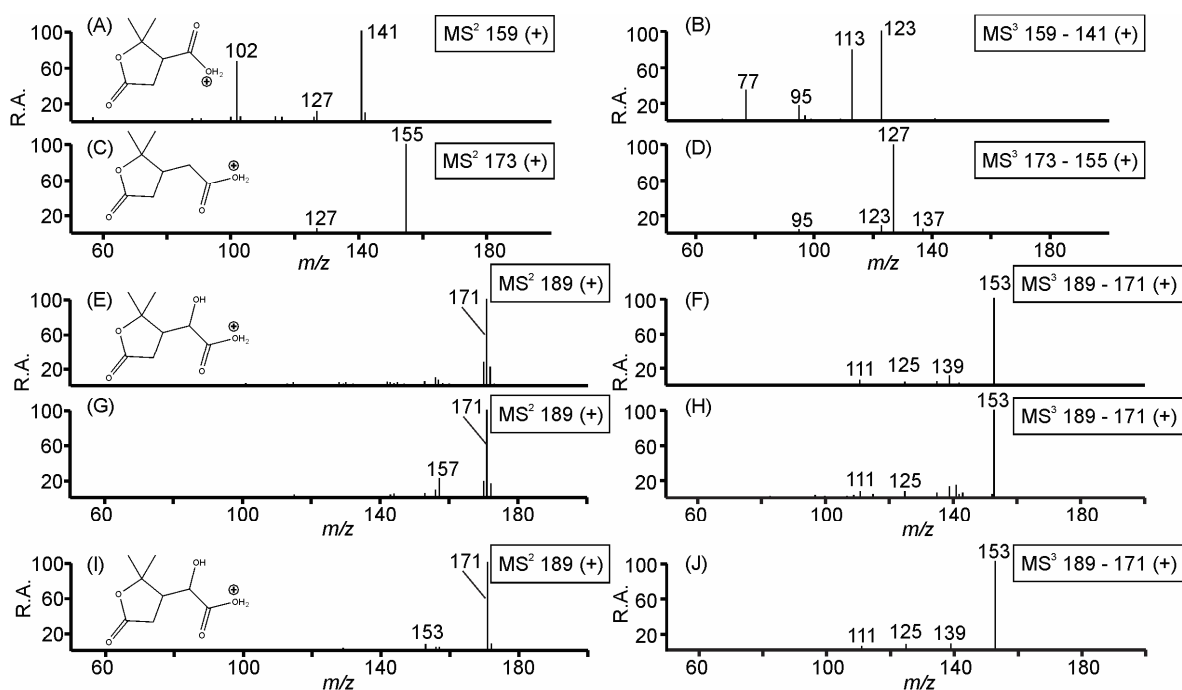


Figure S5. Selected (+)ESI-ITMS data for terebic acid: (A) m/z 159 MS^2 and (B) m/z 159 \rightarrow m/z 141 MS^3 ; terpenylic acid: (C) m/z 173 MS^2 and (D) m/z 173 \rightarrow m/z 155 MS^3 ; the targeted MW 188 compounds present in CAO SOA with RTs 16.3 and 17.0 min: (E, G) m/z 189 MS^2 and (F, H) m/z 189 \rightarrow m/z 171 MS^3 ; and the major MW 188 compound in ambient sample with RT 16.3 min: (I) m/z 189 MS^2 and (J) m/z 189 \rightarrow m/z 171 MS^3 . The retention times for terebic and terpenylic acid under the experimental conditions used for the analysis of the CAO SOA and ambient samples were 17.0 min and 18.7 min, respectively.

S4. Characterization of terebic, terpenylic acid and hydroxyterpenylic acid methyl esters using LC/(+)ESI-ITMS

Figure S6 presents selected MS data for protonated terebic and terpenylic acid methyl esters. Protonated terebic acid methyl ester fragments through the loss of a molecule of water (m/z 155) and methanol (m/z 141), whereas protonated terpenylic acid methyl ester mainly gives rise to the loss of a molecule of water (m/z 169), where the loss of water likely originates in the protonated lactone ring (Fig. S7). In the case of protonated terebic acid methyl ester, further fragmentation of m/z 141 leads to m/z 113 [Fig. S6(B)], corresponding to the loss of CO, whereas fragmentation of m/z 155 mainly results in m/z 123 [Fig. S6(C)], corresponding to the loss of methanol. In the case of protonated terpenylic acid methyl ester, further fragmentation of m/z 169 leads to m/z 141 [Fig. S6(E)], owing to the loss of CO and similar to the behavior of m/z 155 generated from protonated terebic acid methyl ester.

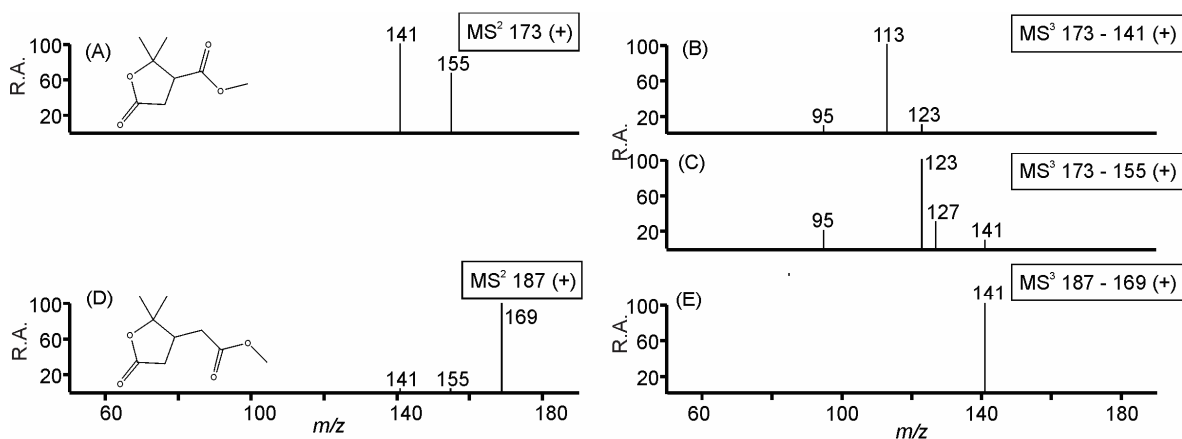


Figure S6. Selected LC/(+)ESI-ITMS data for terebic acid methyl ester: (A) m/z 173 MS^2 , (B) m/z 173 \rightarrow m/z 141 MS^3 , (C) m/z 173 \rightarrow m/z 155 MS^3 ; terpenylic acid methyl ester: (D) m/z 187 MS^2 and (E) m/z 187 \rightarrow m/z 169 MS^3 . The retention times for terebic and terpenylic acid methyl ester were 20.5 min and 21.3 min, respectively.

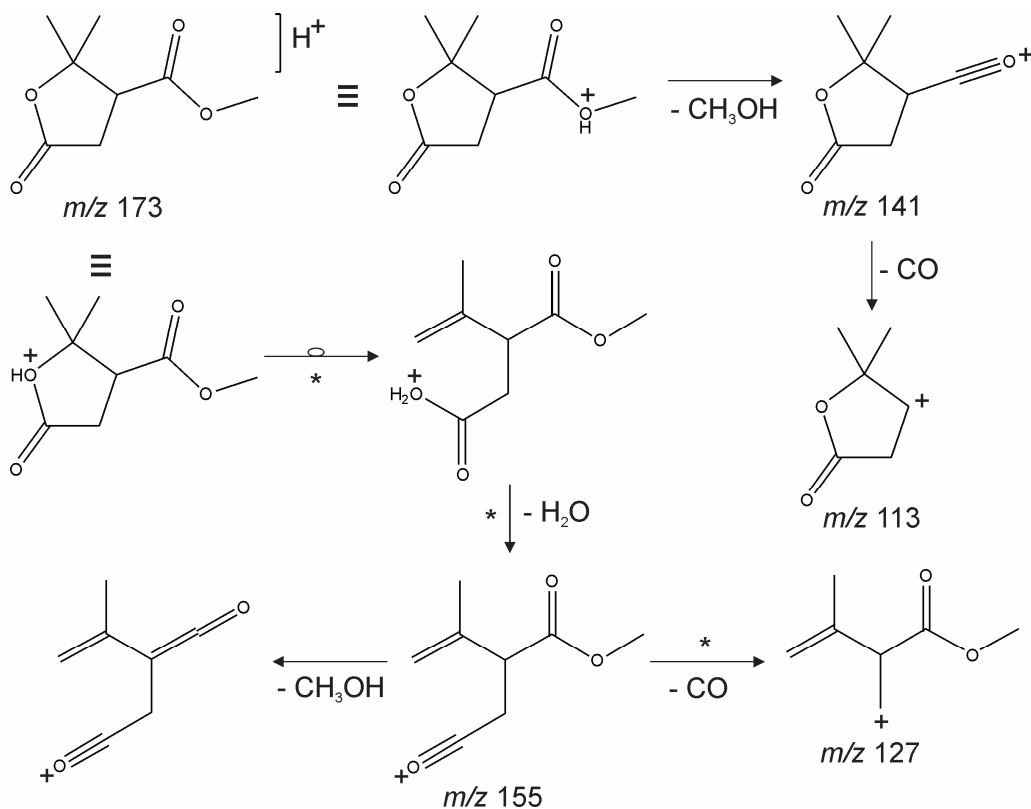


Figure S7. Possible fragmentation pathways for protonated terebic acid methyl ester. The pathways followed by protonated terpenylic acid methyl ester are indicated with an asterisk.

Figures S8 to S11 present selected MS data for methylated MW 188 compounds, which occur in methylated extracts of CAO SOA and the ambient sample. As described in the main text, the MW 202 compounds eluting at 19.1 and 20.5 min (Fig. 2) were assigned to the diastereoisomeric forms of 2-hydroxyterpenylic acid methyl ester and their MS data are shown in Figure S8. Possible fragmentation pathways for protonated 2-hydroxyterpenylic acid methyl ester diastereoisomers are summarized in Figure S9. The compounds eluting at 18.6 and 19.6 min were tentatively attributed to diastereoisomeric forms of 4-hydroxyterpenylic acid methyl ester with corresponding MS data given in Figure S10.

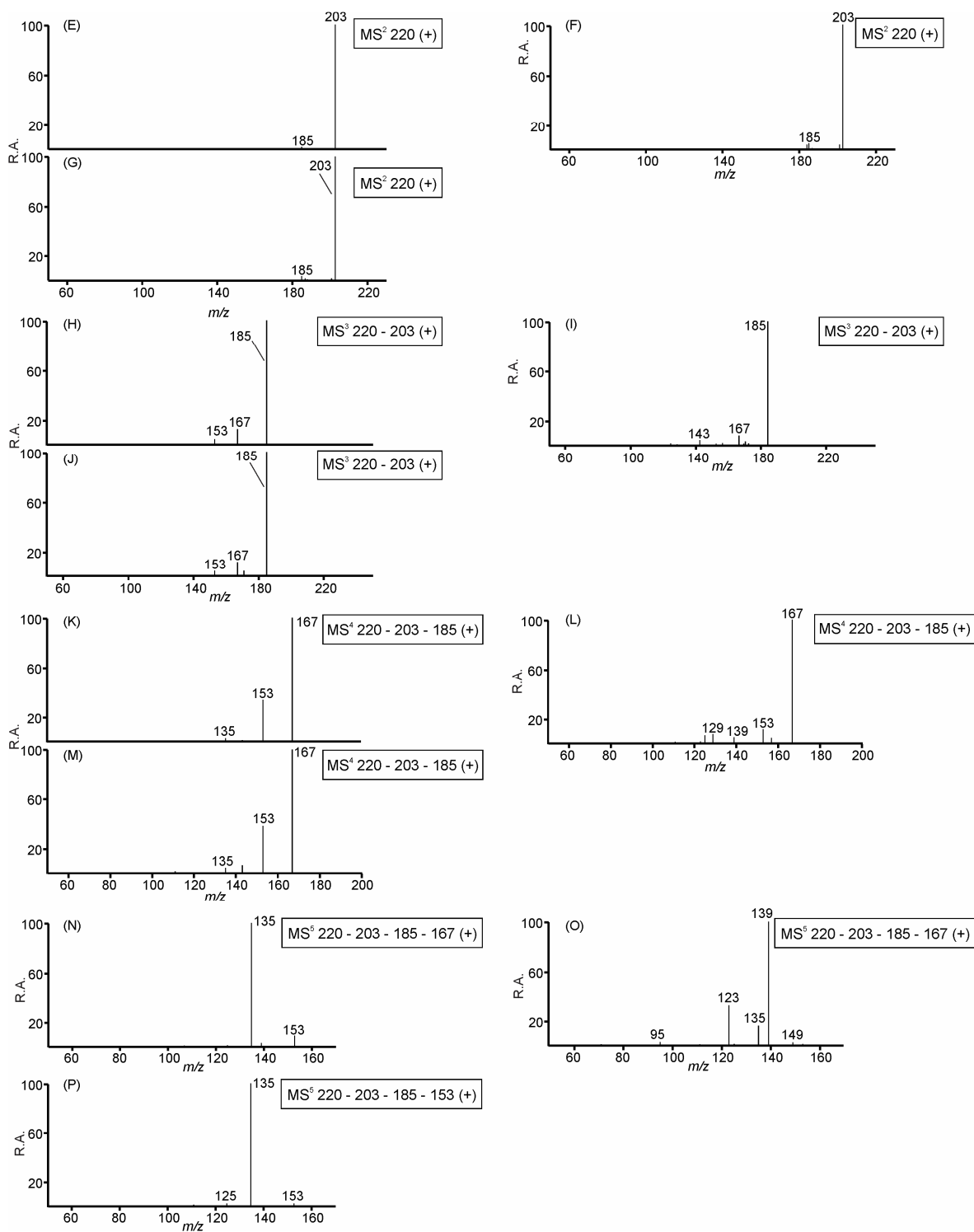


Figure S8. Selected LC/(+)ESI-MS data for the methylated MW 188 compounds assigned to 2-hydroxyterpenylic acid methyl ester diastereoisomers: Product ion spectra are shown in [(E), (K), (N), (P)] for the compound eluting at 19.1 min, and [(F), (I), (L), (O)] for the isomer eluting at 20.5 min in CAO SOA. The corresponding data from the methylated ambient sample are shown in [(G), (J), (M)] for the compound eluting at 19.1 min. Abbreviation: NL, normalization level.

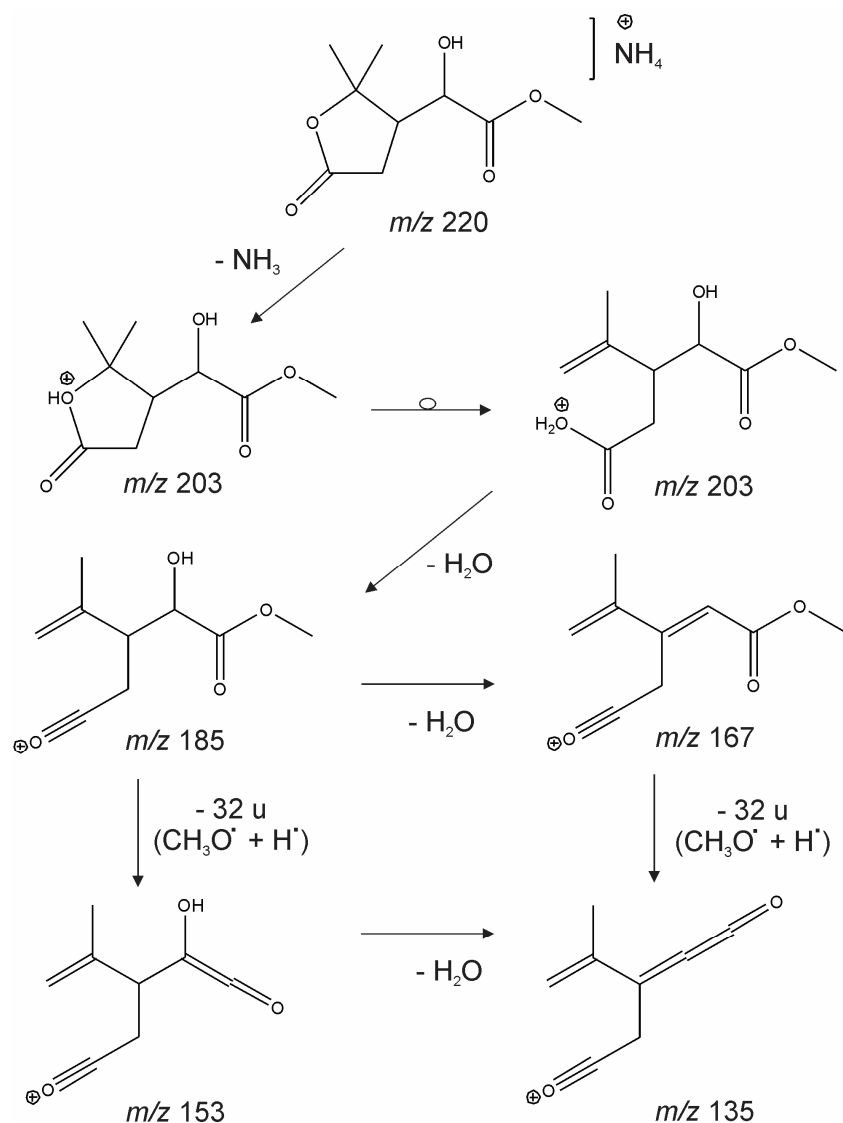


Figure S9. Possible fragmentation pathways for methylated 2-hydroxyterpenylic acid on the basis of LC/(+)ESI-ITMS data.

It can be noted that for the compounds eluting at 18.6 and 19.6 min the m/z 220 MS² spectra only show a minor difference (Fig. S10), i.e., in addition to the protonated molecule at m/z 203 there is a weak m/z 185 owing to the easier subsequent loss of a molecule of water in the first-eluting isomer (18.6 min). Also, the m/z 220 \rightarrow m/z 203 MS³ spectra reveal a minor difference in that in addition to the base peak at m/z 185, corresponding to the loss of water, there is a minor m/z 171 in the first-eluting isomer, owing to the loss of methanol. It can be seen that the m/z 220 \rightarrow m/z 203 \rightarrow m/z 185 MS⁴ spectrum obtained from the compound

eluting at 18.6 min [Fig. S10(A, D, G)] is distinctly different from that eluting at 19.6 min [Fig. S10(B, E, H)]. Possible fragmentation pathways for the MW 202 compound eluting at 18.6 min, assigned to 4-hydroxyterpenylic acid methyl ester, are summarized in Figure S11. The observed neutral losses of 88, 74, 60 and 32 *u* can be explained with a 4-hydroxyterpenylic acid methyl ester structure.

Although the abundance of this positional isomer is smaller than that of 2-hydroxyterpenylic acid, it has atmospheric relevance as it could also be observed from the methylated K-pusztá sample [Fig. S10(C, F, I)]. As already mentioned in the main text, the corresponding non-methylated form of 4-hydroxyterpenylic acid was not observed in the current study from the CAO SOA sample but a compound possibly corresponding to it has been detected in a previous study by Yasmeen et al. (5), i.e., the MW 188 compound eluting at 13.2 min under comparable chromatographic conditions (Fig. A4 in the cited study). The deprotonated form of the latter compound revealed a product ion at *m/z* 59 in a *m/z* 187 → *m/z* 143 MS³ experiment (Fig. A4 in the cited article) which is in agreement with the carboxymethyl side chain. Furthermore, two early-eluting MW 188 compounds were also noted in a previous study by Claeys et al. (1) both in ambient aerosol and α-pinene SOA, i.e., compounds with RTs between 13 and 14 min [Fig. 1(A) and (B) in the cited study]. The two compounds likely correspond to diastereoisomeric forms with 3*S*,4*R* and 3*S*,4*S* configurations with estimated dipole moments 2.9, 4.4, 4.5 and 3.9, 5.4, 5.4 D for the gas phase, methanol and water, respectively.

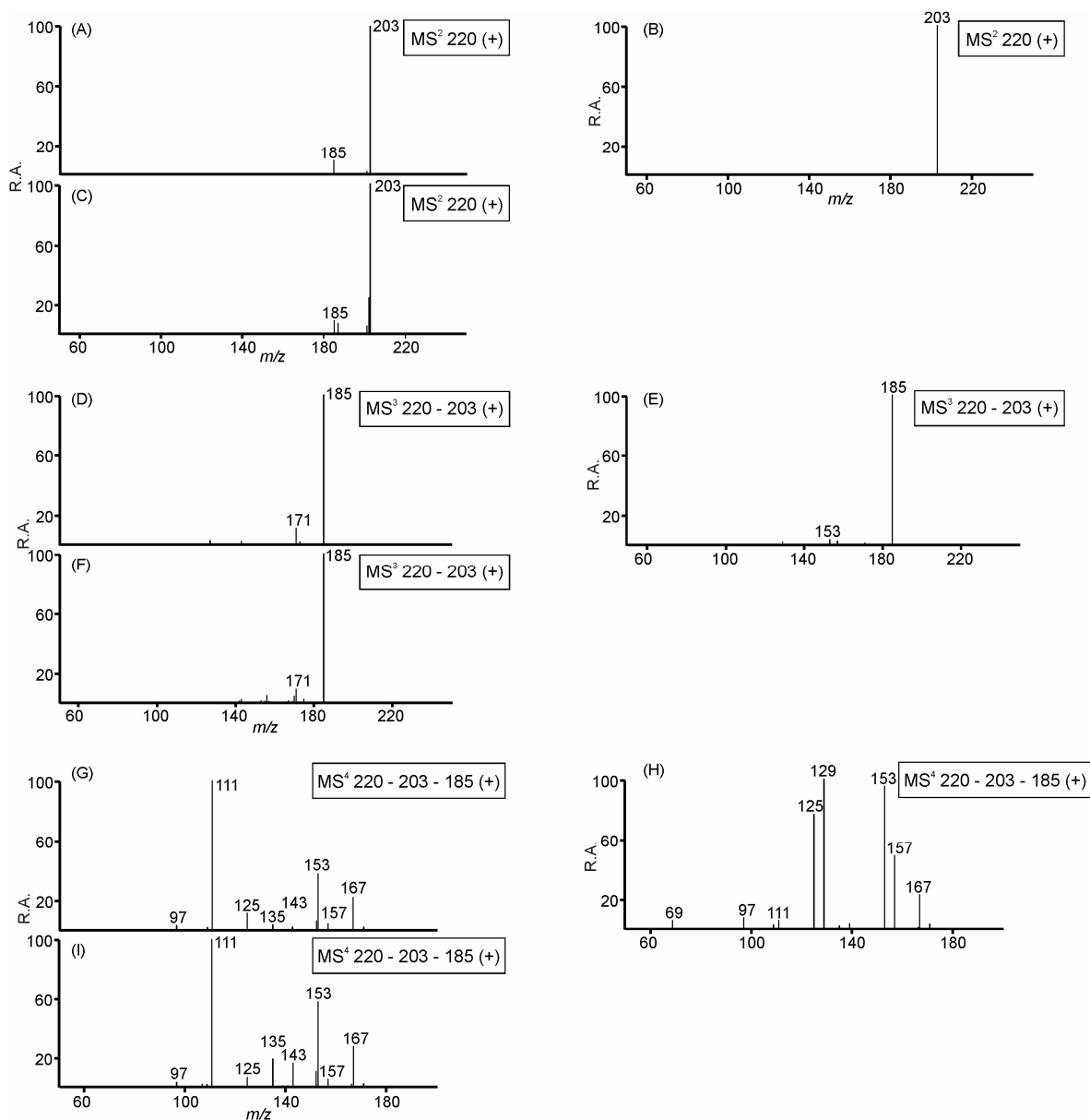


Figure S10. Selected LC/(+)ESI-ITMS data for the methylated MW 188 compounds, attributed to methylated 4-hydroxyterpenylic acid diastereoisomers, present in methylated extracts of CAO SOA (A, D, G), for the compound eluting at 18.6, and (B, E, H) for the isomer eluting at 19.6 min. Data from the ambient sample are shown in (C, F, I) for the compound eluting at 18.6 min. The methylated MW 188 compounds were detected as their ammonium adduct ions at m/z 220.

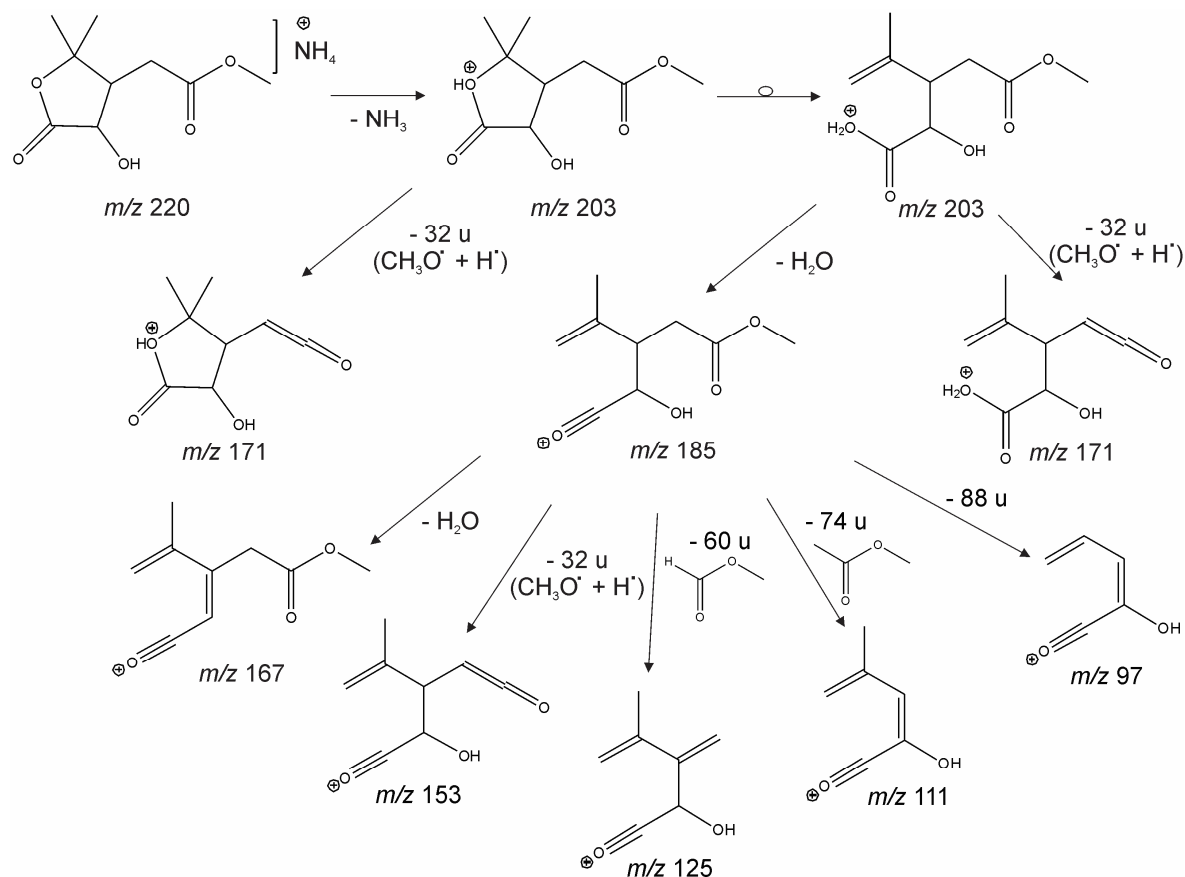


Figure S11. Possible fragmentation pathways for 4-hydroxyterpenylic acid methyl ester.

S5. Characterization of terebic, terpenylic acid and hydroxyterpenylic acid methyl esters using GC/(+)EI-MS

Figure S12 presents selected MS data for protonated terebic and terpenylic acid methyl esters from electron impact (EI) GC/MS analysis. The first-order EI mass spectrum for the terebic acid methyl ester is dominated by m/z 129, which results from the loss of a methyl radical and an additional loss of CO [Fig. S12(B)]. In contrast, the m/z 139 is the most abundant product ion for terpenylic acid methyl ester, which corresponds to the loss of a methyl radical and an additional loss of methanol [Fig. S12(F)]. Further fragmentation studies of these main product ions [Fig. S12(C) and (G)], as well of the product ions that correspond to the methyl radical loss [Fig. S12(D) and (H)] reveal a specific fragmentation behavior owing to the difference in the length of the side chain. The proposed fragmentation mechanisms are given in Figures S13 and S14 for terebic and terpenylic acid methyl ester, respectively.

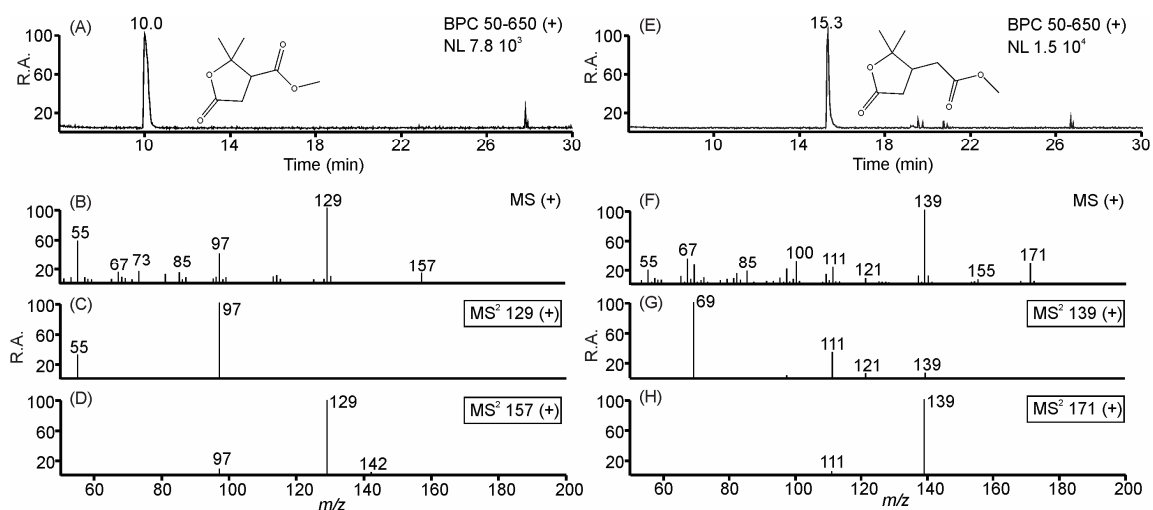


Figure S12. Base Peak Chromatograms (BPCs) of methylated standard compounds and selected MS data from GC/(+)EI-MS analysis: (A-D) terebic acid methyl ester, (E-H) terpenylic acid methyl ester. Abbreviation: NL, normalization level.

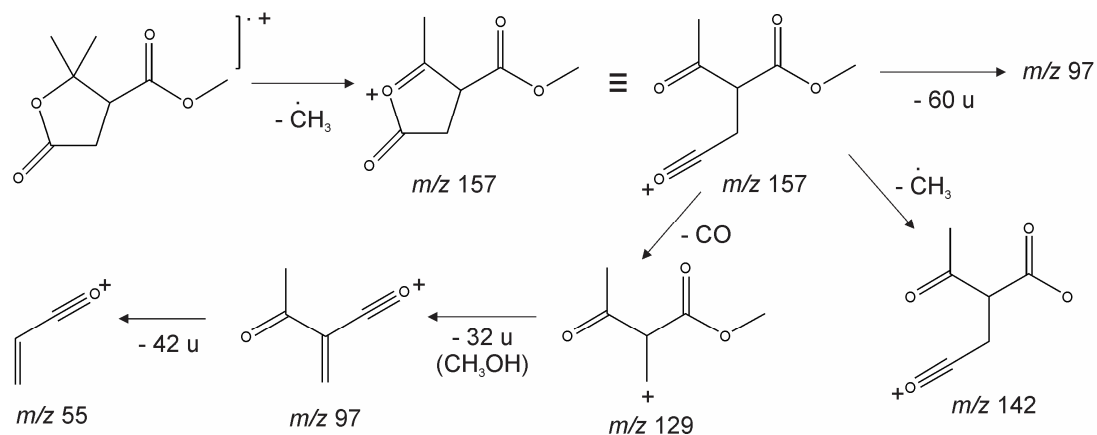


Figure S13. Possible fragmentation pathways for terebic acid methyl ester based on GC/(+)EI-MS data.

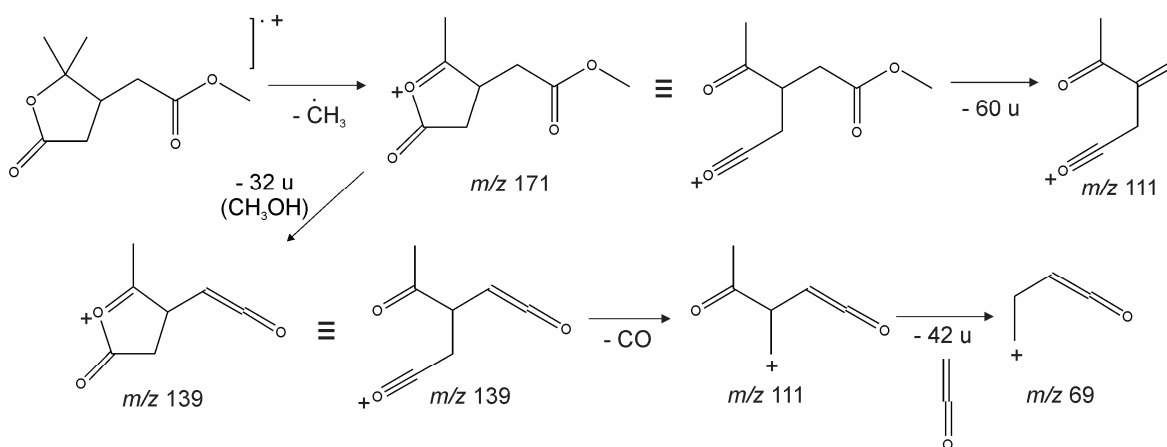


Figure S14. Possible fragmentation pathways for terpenylic acid methyl ester based on GC/(+)EI-MS data.

Selected mass spectral data from the GC/(+)EI-MS analysis of the proposed methylated 2-hydroxyterpenylic acid diastereoisomers in the CAO SOA sample and the ambient sample are shown in Figure S15. Based on the detailed interpretation of the EI-MS data, the structure of 2-hydroxyterpenylic acid methyl ester was supported, as shown in Figure S16.

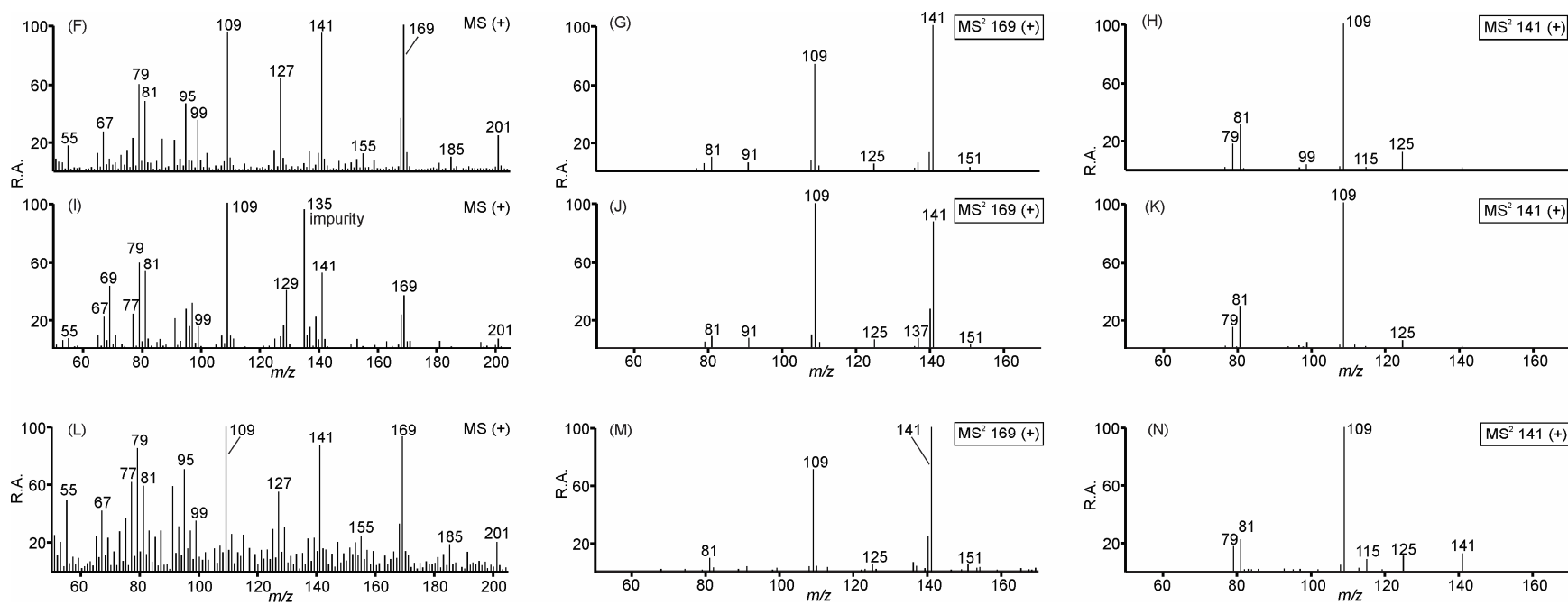


Figure S15. Selected GC/(+)EI-MS data for methylated MW 188 compounds present in CAO SOA eluting at 21.1 min (F-H) and 20.6 min (I-K), and corresponding data for the ambient sample for the isomer detected at 21.1 min (L-N).

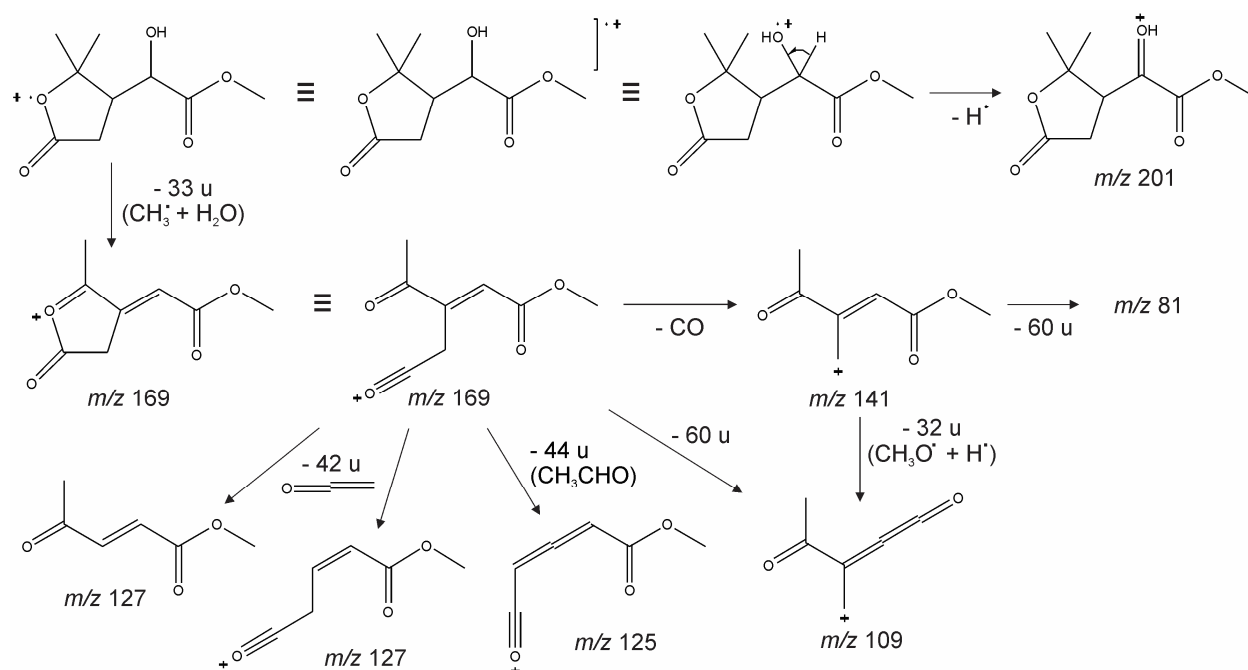


Figure S16. Possible fragmentation pathways for methylated 2-hydroxyterpenylic acid on the basis of GC/(+)EI-MS data.

REFERENCES

- (1) Claeys, M.; Iinuma, Y.; Szmigielski, R.; Surratt, J. D.; Blockhuys, F.; Van Alsenoy, C.; Böge, O.; Sierau, B.; Gómez-González, Y.; Vermeylen, R.; Van der Veken, P.; Shahgholi, M.; Chan, A. W. H.; Herrmann, H.; Seinfeld, J. H.; Maenhaut, W. Terpenylic acid and related compounds from the oxidation of α -pinene: Implications for new particle formation and growth above forests. *Environ. Sci. Technol.* **2009**, *43*, 6976–6982.
- (2) Van den Bergh, V.; Vanhees, I.; De Boer, R.; Compennolle, F.; Vinckier, C. Identification of the oxidation products of the reaction between α -pinene and hydroxyl radicals by gas and high-performance liquid chromatography with mass spectrometric detection. *J. Chromatogr. A* **2000**, *896*, 135–148.
- (3) Iinuma Y.; Kahnt, A.; Mutzel, A.; Böge, O.; Herrmann, H. Ozone-driven secondary aerosol production chain. *Environ. Sci. Technol.* **2013**, *47*, 3639–3647.
- (4) Kahnt, A.; Iinuma Y.; Mutzel, A.; Böge, O.; Claeys, M.; Herrmann, H. Campholenic aldehyde ozonolysis: a mechanism leading to specific biogenic secondary organic aerosol constituents. *Atmos. Chem. Phys.* **2014**, *14*, 719–736.
- (5) Yasmeeen, F.; Szmigielski, R.; Vermeylen, R.; Gómez-González, Y.; Surratt, J. D.; Chan, A. W. H.; Seinfeld, J. H.; Maenhaut, W.; Claeys, M. Mass spectrometric characterization of isomeric terpenoic acids from the oxidation of α -pinene, β -pinene, *d*-limonene, and Δ^3 -carene in fine forest aerosol. *J. Mass Spectrom.* **2011**, *46*, 425–442.